

SCIENTIFIC REPORTS

OPEN

Anomalous random telegraph noise in nanoscale transistors as direct evidence of two metastable states of oxide traps

Shaofeng Guo, Runsheng Wang, Dongyuan Mao, Yangyuan Wang & Ru Huang

In this paper, a new pattern of anomalous random telegraph noise (RTN), named “reversal RTN” (rRTN) induced by single oxide trap, is observed in the drain current of nanoscale metal-oxide-semiconductor field-effect transistors (MOSFETs) with high- k gate dielectrics. Under each gate voltage, the rRTN data exhibit two zones with identical amplitudes but reversal time constants. This abnormal switching behavior can be explained by the theory of complete 4-state trap model (with two stable states and two metastable states), rather than the simple 2-state or improved 3-state trap model. The results provide a direct experimental evidence of the existence of two metastable states in a single oxide trap, contributing to the comprehensive understanding of trap-related reliability and variability issues in nanoscale transistors.

With the metal-oxide-semiconductor field-effect transistor (MOSFET) dimension downscaling, oxide traps in the gate dielectric have drawn much attention due to their serious impacts on the device reliability and variability^{1–11}. The random charging/discharging processes of traps have been studied directly based on the random telegraph noise (RTN) in the drain current of MOSFETs^{1,7}. Normally, the single-trap induced RTN is a typical Poisson process⁷, as illustrated in Fig. 1. The stochastic trapping/detrapping behavior can be characterized by two parameters: capture time constant (τ_c) and emission time constant (τ_e), representing the average waiting time to capture (or emit) a carrier from (or to) the channel⁷.

Apart from the normal RTN, two patterns of the anomalous temporary RTN (tRTN) induced by single oxide trap with two current levels have been reported^{12,13}, as also illustrated in Fig. 1, where the fast switching process can suddenly appear or disappear. Both patterns can be explained by the 3-state trap model^{12,13}, improved from the simple 2-state trap model by including one additional metastable trap state. The “quiet” phases with no switching behaviors correspond to the transition between the neutral state (1) and the neutral metastable state (1'). In order to describe the trap-induced reliability physics of bias temperature instability (BTI) in MOSFETs, recently, the complete 4-state trap model⁷ with two metastable states has also been proposed and verified with indirect proofs^{7,14,15}, but was lack of direct evidence from RTN. In this paper, a new pattern of anomalous RTN in nanoscale MOSFETs is observed and analyzed in detail, providing a direct support on the complete 4-state trap model.

Experimental Results

Devices characterized in this work are planar high- k /metal-gate n-type MOSFETs with length $L = 60$ nm, width $W = 300$ nm and ultra-thin HfO_2 gate dielectrics. The experimental results of the anomalous RTN in drain current under different gate voltages V_G are shown in Fig. 2, with the drain voltage kept at $V_D = 50$ mV, and temperature $T = 25$ °C. For other V_G , the anomalous RTN data are shown in Fig. S1 of the supplementary materials. It can be clearly observed that this RTN exhibits two zones (zone A & zone B) under the same bias. The results are repeatable after measurement interruptions. As illustrated in Fig. 3, the expanded detail shows that the capture time constant is smaller than the emission time constant in zone A, while it has the reversal feature in zone B. Therefore, it is named “reversal RTN” (rRTN) here.

To have quantitative information, the characteristics of the rRTN in zone A and zone B are carefully investigated in the following three aspects: amplitudes, time constants and trap position. The extracted amplitudes of RTN in zone A and B are shown in Fig. 4(a), which are identical under different V_G , indicating that the rRTN has

Institute of Microelectronics, Peking University, Beijing, 100871, China. Correspondence and requests for materials should be addressed to R.W. (email: r.wang@pku.edu.cn)

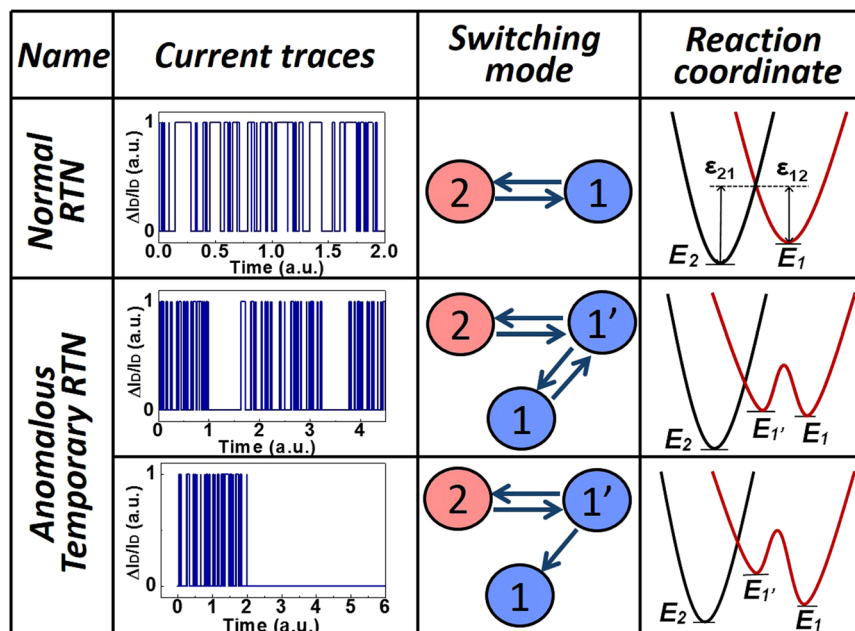


Figure 1. The illustrations of the current traces, switching modes and the corresponding reaction coordinate of the normal RTN and two patterns of anomalous temporary RTN^{9,10} (tRTN), where state 2 is charged state, and state 1 and metastable state 1' are neutral state.

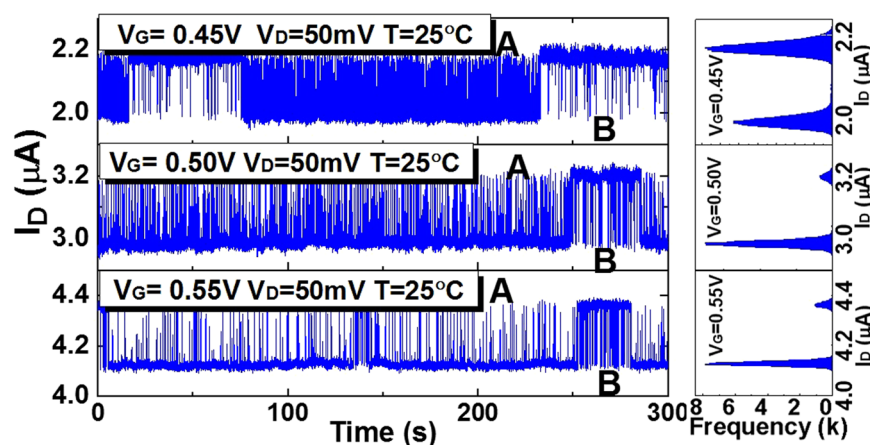


Figure 2. Left: Experimental results of the rRTN in the drain current of the nanoscale MOSFET under three different gate voltages. The rRTN trace exhibits two zones with different time constants. The average transition time between zone A and zone B is hundreds of seconds. Right: The histograms of the RTN data at different V_G , indicating the two current levels.

only two current levels throughout the entire time domain. In principle, the RTN induced by N traps in a single device should be corresponding to 2^N current levels. Therefore, it is most likely that zone A and zone B represent the same trap, otherwise, there should be more than two current levels due to the superposition of RTN levels induced by more than one traps. The time constants τ_c and τ_e in each zone are extracted as shown in Fig. 4(b), and the extraction details are shown in Fig. S2 of the supplementary materials. Both τ_c and τ_e in two zones have the similar V_G dependence, respectively. Therefore, based on the relationship^{16,17}

$$\frac{x}{T_{OX}} = -\frac{k_B T}{q} \frac{\partial \ln(\tau_c/\tau_e)}{\partial V_G} \quad (1)$$

$$T_{OX} = T_{IL} + \frac{\epsilon_{SiO_2}}{\epsilon_{HK}} T_{HK} \quad (2)$$

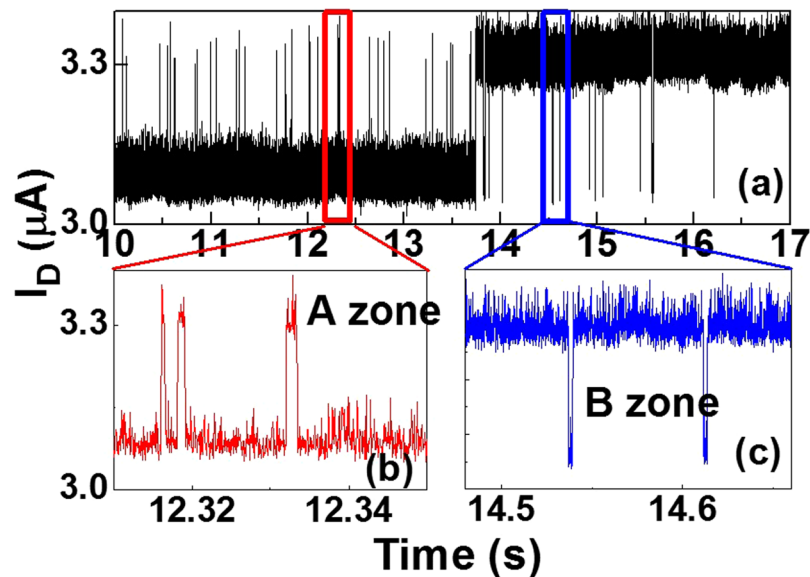


Figure 3. A closer view of the rRTN under $V_G = 0.5$ V in zone A and zone B separately. The emission time constant ($\bar{\tau}_e$) in zone A is larger than the capture time constant ($\bar{\tau}_c$), while $\bar{\tau}_c$ is larger in zone B.

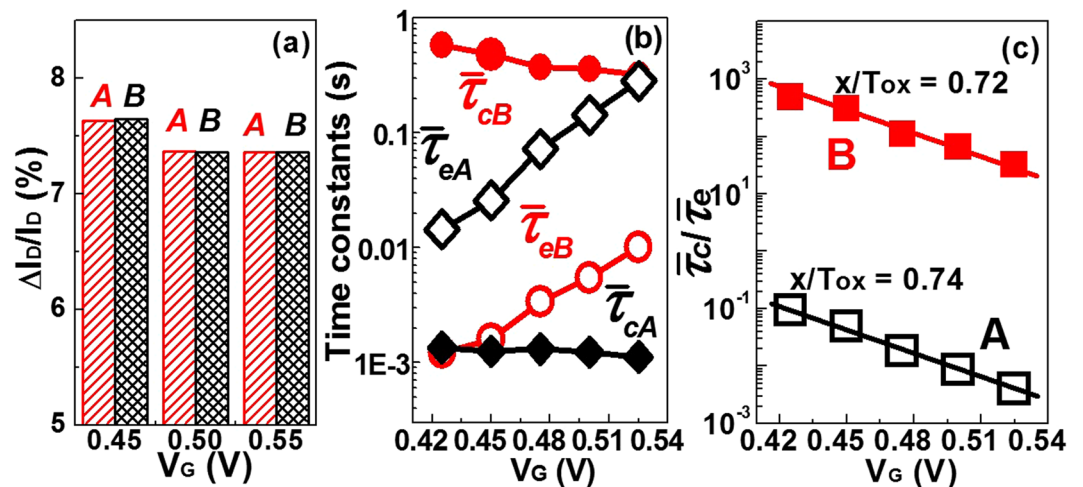


Figure 4. The comparisons of (a) amplitudes, (b) time constants and (c) the extracted trap position in zone A and zone B. The results suggest that zone A and zone B represent the same single oxide trap in the gate dielectric.

where T_{IL} is the thickness of the SiO_2 interfacial layer and T_{HK} the thickness of the HfO_2 high-k layer, ϵ_{SiO_2} and ϵ_{HK} are the dielectric constants for SiO_2 and the HfO_2 high-k dielectric, respectively, k_B is the Boltzmann constant and T is the temperature, the vertical distance x to the oxide/channel interface can be attained. It is worth mentioning that since the RTN measurement region is above the threshold voltage in this work, the effect of $\partial\psi_s/\partial V_{GS}$ is small and thus is ignored for simplicity¹⁸. As shown in Fig. 4(c), the x/T_{Ox} extracted from two zones are 0.74 and 0.72, respectively, which are almost the same, suggesting the same trap location in the HfO_2 dielectric, thus providing another proof that two zones correspond to one single trap.

Discussions on Physical Mechanism

It is believed that, during the transition from one valence state to another, the trap may go through a metastable state^{1,7,14}. In order to explain the mechanism of rRTN with two zones, all the possible trap models, i.e., 2-state, 3-state (with one metastable state) and 4-state (with two metastable states) trap models, are studied. First, the simple 2-state trap model originating from the normal RTN theory can be excluded apparently, because metastable states should be introduced to interpret the abnormal switching phenomenon. Next, the 3-state trap model with one additional metastable state is considered. It is worth noting that the 3-state trap model as shown in Fig. 1 cannot explain the rRTN, due to the fact that the switching phenomenon in rRTN is frequent throughout the

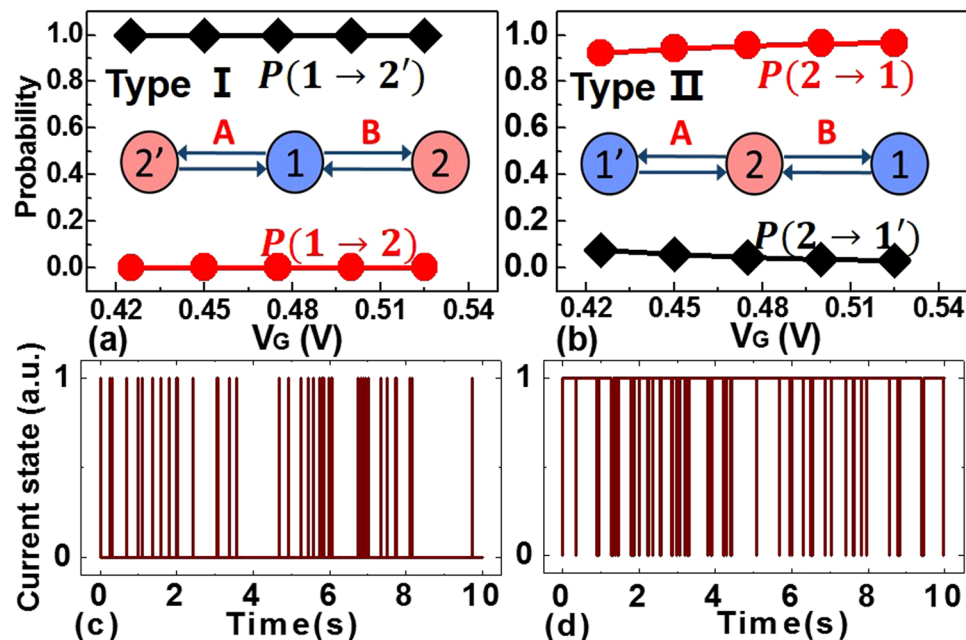


Figure 5. (a,b) Illustration of the transition probabilities between different states in two types (type I and type II) of the 3-state trap model, where the state 2 and metastable state $2'$ are the charged states and the state 1 and metastable state $1'$ are neutral states. (c,d) Theoretical simulated RTN results based on the extracted time constants with two types of 3-state trap model under $V_G = 0.425$ V.

entire time domain with no “quiet” phase. Therefore, the 3-state trap model needs to be modified. There are two types of 3-state trap model can be the candidate transition modes, as shown in the inserted of Fig. 5(a,b). Based on the extracted time constants from these two zones, the transition probabilities between each two states can be calculated as follows:

For the type I:

$$P(1 \rightarrow 2) = \frac{\bar{\tau}_{12'}}{\bar{\tau}_{12} + \bar{\tau}_{12'}} \quad (3)$$

$$P(1 \rightarrow 2') = \frac{\bar{\tau}_{12}}{\bar{\tau}_{12} + \bar{\tau}_{12'}} \quad (4)$$

For the type II:

$$P(2 \rightarrow 1) = \frac{\bar{\tau}_{21'}}{\bar{\tau}_{21} + \bar{\tau}_{21'}} \quad (5)$$

$$P(2 \rightarrow 1') = \frac{\bar{\tau}_{21}}{\bar{\tau}_{21} + \bar{\tau}_{21'}} \quad (6)$$

The extracted transition probabilities under different V_G are shown in Fig. 5(a,b). For the type I model, it can be found that $P(1 \rightarrow 2')$ is about 1, and $P(1 \rightarrow 2)$ is close to 0. It can be deduced that if the transition from state 2 to 1 is very fast, the probabilities will lead to almost the same results as normal RTN with two current levels. If the transition from 2 to 1 is slow, there will be a long time period when the current is staying at the low level. Based on the extracted time constants, the RTN simulation with multiple states can be performed. The details of the theoretical simulation method are shown in Figs S3 and S4 in the supplementary materials, which is similar to ref. 19. The result is shown in Fig. 5(c). As expected, the 3-states model of type I are inconsistent with the experimental results. Similarly, the type II model also fails to interpret the experimental rRTN results, which is verified by the simulated RTN result shown in Fig. 5(d).

Last, the complete 4-state trap model with two metastable trap states is examined, as shown in Fig. 6(a), including one neutral metastable state ($1'$) and one charged metastable states ($2'$). Zone A corresponds to the switching process between state $1'$ and state 2, and zone B is between state 1 and state $2'$. It is worth mentioning that the transition probabilities of $1 \rightarrow 1'$ (or $2 \rightarrow 2'$) is usually smaller compared with other transition processes, due to higher barrier $\varepsilon_{11'}$ (or $\varepsilon_{22'}$) than others. Therefore, in previously reported experiments, it is rare to observe RTN data featuring the transitions among four states. Regarding the rRTN observed in this paper, particularly, the 4-state trap model can be described in the reaction coordinate as shown in Fig. 6(b). The transition barriers should follow these relationships: $\varepsilon_{12'} < \varepsilon_{11'}$ and $\varepsilon_{21} < \varepsilon_{22'}$, otherwise, there is only single zone, as illustrated based

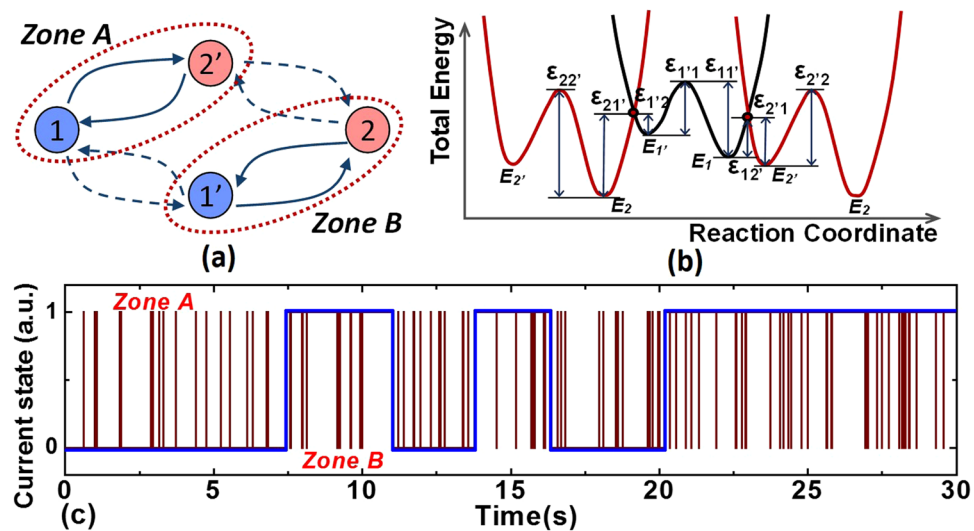


Figure 6. (a) Illustration of the complete 4-state model. The zone A and zone B in rRTN correspond to the transition processes in circles. (b) Schematic of the corresponding reaction coordinate of the complete 4-state trap model. (c) Theoretical simulated RTN results based on the extracted time constants associated with the complete 4-state trap model, which are consistent with the experimental results in Fig. 2.

on the simulated RTN results in Fig. S5 of the supplementary materials. Therefore, the switching between $1 \leftrightarrow 2'$ (or, $2 \leftrightarrow 1'$) are preferred rather than between $1 \leftrightarrow 1'$ (or, $2 \leftrightarrow 2'$). Once the trap state turns to the zone A, it will stay in this zone for a period until the state turns to $1'$ via 1 (or, to 2 via $2'$). Similarly, it can also stay in the zone B for a period until the trap state turn to 1 via $1'$ (or, to $2'$ via 2). In other words, the fast switching zones A and B can appear randomly with a lasting time longer than the average transition time, which is exactly consistent with the observed rRTN. Based on the extracted time constants, the simulated RTN result with the 4-state trap model can be obtained, as shown in Fig. 6(c), which is consistent with the rRTN experimental results. Finally, it can be concluded that the experimental results can only be explained by the 4-state trap model (with two metastable states), rather than the simple 2-state trap model (without metastable states) and the improved 3-state model (with one metastable state). In addition, as mentioned earlier, if the trap exhibits four states rather than two states, it can affect the frequency dependence of BTI reliability^{15,20,21}, which is still under investigation.

Conclusion

In summary, single-trap induced rRTN with two evident zones is observed in nanoscale transistors with HfO_2 gate oxide. Based on the analysis of transition probabilities and the corresponding simulated RTN results, the abnormal transition mechanism can be explained by the complete 4-state trap model, thus directly verifying the existing of two metastable states at single-trap based on the experimental results, which is helpful for comprehensive understanding of trap-related device reliability and variability physics.

References

- Kirton, M. J. & Uren, M. J. Noise in solid-state microstructures: A new perspective on individual defects, interface states and low-frequency ($1/f$) noise. *Adv. in Phys.* **38**, 367–468 (1989).
- Zhuge, J. *et al.* Random telegraph signal noise in gate-all-around silicon nanowire transistors featuring coulomb-blockade characteristics. *Appl. Phys. Lett.* **94**, 083503 (2009).
- Grasser, T., Reisinger, H., Wagner, P.-J. & Kaczer, B. Time-dependent defect spectroscopy for characterization of border traps in metal-oxide-semiconductor transistors. *Phys. Rev. B* **82**, 245318 (2010).
- Kaczer, B., Roussel, Ph. J., Grasser, T. & Groeseneken, G. Statistics of multiple trapped charges in the gate oxide of deeply scaled MOSFET devices—application to NBTI. *IEEE Electron Device Lett.* **31**, 411–413 (2010).
- Clement, N., Nishiguchi, K., Fujiwara, A. & Vuillaume, D. One-by-one trap activation in silicon nanowire transistor. *Nat. Commun.* **1**, 92, doi:10.1038/ncomms1092 (2010).
- Ren, P. *et al.* Experimental study on the oxide trap coupling effect in metal oxide semiconductor field effect transistors with HfO_2 gate dielectrics. *Appl. Phys. Lett.* **104**, 263512 (2014).
- Grasser, T. Stochastic charge trapping in oxides: from random telegraph noise to bias temperature instabilities. *Microelectron. Reliab.* **52**, 39–70 (2012).
- Wang, R. *et al.* A unified approach for trap-aware device/circuit co-design in nanoscale CMOS technology. In IEEE Int. Electron Devices Meet. *Tech. Dig.* **2013**, 834–837, doi:10.1109/IEDM.2013.6724745 (2013).
- Yu, B. *et al.* Design for manufacturability and reliability in extreme-scaling VLSI. *Sci. China Inf. Sci.* **59**, 061406 (2016).
- Delfonibus, S. Looking into the future of nanoelectronics in the diversification efficient era. *Sci. China Inf. Sci.* **59**, 061401 (2016).
- Zou, J., Guo, S., Huang, R. & Wang, R. AC random telegraph noise (AC RTN) in nanoscale MOS devices in *outlook and challenges of nano devices, sensors, and MEMS* (ed. Li, T. and Liu, Z.) 99–122 (Springer, 2017).
- Uren, M. J., Kirton, M. J. & Collins, S. Anomalous telegraph noise in small-area silicon metal-oxide-semiconductor field-effect transistors. *Phys. Rev. B* **37**, 8346 (1988).
- Grasser, T. *et al.* The time dependent defect spectroscopy (TDDS) for the characterization of the bias temperature instability. *Int. Reliab. Phys. Symp. Proc.* **2010**, 16–25, doi:10.1109/IRPS.2010.5488859 (2010).
- Grasser, T. *et al.* On the microscopic structure of hole traps in pMOSFETs. In IEEE Int. Electron Devices Meet. *Tech. Dig.* **2014**, 530–533, doi:10.1109/IEDM.2014.7047093 (2014).

15. Mao, D., Guo, S., Wang, R., Liu, C. & Huang, R. On the origin of frequency dependence of single-trap induced degradation in AC NBTI. *Int. Symp. on the Physical and Failure Analysis of Integrated Circuits (IPFA)* **2015**, 107–110, doi:[10.1109/IPFA.2015.7224344](https://doi.org/10.1109/IPFA.2015.7224344) (2015).
16. Celik-Butler, Z., Vasina, P. & Amarasinghe, N. V. A method for locating the position of oxide traps responsible for random telegraph signals in submicron MOSFET's. *IEEE Trans. Electron Devices* **47**, 646 (2000).
17. Li, Y. *et al.* Random-telegraph-signal noise in AlGaIn/GaN MIS-HEMT on silicon. *Electron. Lett.* **49**, 156 (2012).
18. Nour, M. *et al.* A stand-alone, physics-based, measurement-driven model and simulation tool for random telegraph signals originating from experimentally identified MOS gate-oxide defects. *IEEE Trans. Electron Devices* **63**, 1428 (2016).
19. Martin-Martinez, J. *et al.* Probabilistic defect occupancy model for NBTI. *Int. Reliab. Phys. Symp. Proc.* **2011**, 920–925, doi:[10.1109/IRPS.2011.5784605](https://doi.org/10.1109/IRPS.2011.5784605) (2011).
20. Mao, D., Guo, S., Wang, R., Huang, R. & Liu, C. Impacts of metastable defect states on gate oxide trapping in nanoscale MOS devices. *Int. Nanoelectronics Conf. (INEC)* 1–2, doi:[10.1109/INEC.2016.7589302](https://doi.org/10.1109/INEC.2016.7589302) (2016).
21. Grasser, T. *et al.* On the microscopic origin of the frequency dependence of hole trapping in pMOSFETs. In *IEEE Int. Electron Devices Meet. Tech. Dig.* **2012**, 470–473, doi:[10.1109/IEDM.2012.6479076](https://doi.org/10.1109/IEDM.2012.6479076) (2012).

Acknowledgements

This work was partly supported by NSFC (61522402 and 61421005) and 863 Project (2015AA016501). The authors would like to thank Xiaobo Jiang for the helpful discussions.

Author Contributions

R.W. and R.H. supervised the project, S.G. and R.W. conceived the experiment, S.G. conducted the experiment and wrote the main manuscript text, S.G., R.W. and D.M. analyzed the experimental data, R.W., Y.W. and R.H. contributed to the paper writing. All authors reviewed the manuscript.

Additional Information

Supplementary information accompanies this paper at doi:[10.1038/s41598-017-06467-7](https://doi.org/10.1038/s41598-017-06467-7)

Competing Interests: The authors declare that they have no competing interests.

Publisher's note: Springer Nature remains neutral with regard to jurisdictional claims in published maps and institutional affiliations.



Open Access This article is licensed under a Creative Commons Attribution 4.0 International License, which permits use, sharing, adaptation, distribution and reproduction in any medium or format, as long as you give appropriate credit to the original author(s) and the source, provide a link to the Creative Commons license, and indicate if changes were made. The images or other third party material in this article are included in the article's Creative Commons license, unless indicated otherwise in a credit line to the material. If material is not included in the article's Creative Commons license and your intended use is not permitted by statutory regulation or exceeds the permitted use, you will need to obtain permission directly from the copyright holder. To view a copy of this license, visit <http://creativecommons.org/licenses/by/4.0/>.

© The Author(s) 2017